Null-Space Compliance Variation for Safe Human-Robot Collaboration in Redundant Manipulators using Safety Control Barrier Functions

Salt Ducaju, Julian; Olofsson, Björn; Robertsson, Anders; Johansson, Rolf

Published in:
Proc. 2023 IEEE/RSJ International Conference on Intelligent Robots and Systems (IROS 2023)

DOI:
10.1109/IROS55552.2023.10342181

2023

Document Version:
Peer reviewed version (aka post-print)

Null-Space Compliance Variation for Safe Human-Robot Collaboration in Redundant Manipulators using Safety Control Barrier Functions

Julian M. Salt Ducaju, Björn Olofsson, Anders Robertsson, Rolf Johansson

***Abstract*— In this paper, Safety Control Barrier Functions (SCBFs) were used to adjust the null-space compliant behavior of a redundant robot to improve safety in Human–Robot Collaboration (HRC) without modifying the robot behavior with respect to its main Cartesian task. A Lyapunov function was included in an energy storage formulation compatible with strict passivity to provide global asymptotic stability guarantees for the null-space compliance variation, and the necessary conditions for stability were formulated as inequality constraints of the optimization problem used for the null-space compliance variation. Experimental validation was performed using a Franka Emika Panda robot for a collaborative assembly application and its results showed that safety can be improved by using SCBFs simultaneously to the optimization of the robot configuration, while employing a single degree of freedom.**

I. Introduction

The recent interest in the manufacturing industry to replace mass production for mass customization has caused an increase in the relevance of Human–Robot Collaboration (HRC) in the robotics community [1]. Human operators can use their intelligence and dexterity to increase flexibility in robotic manufacturing and to decrease the complexity of the robot tools, while robots can reduce the operator fatigue, *e.g.*, in industries, such as aeronautics, where assembly applications are still mainly manual as a result of their complexity [2].

Human safety is a requirement of collaborative applications. A control strategy often used for human collaboration is impedance control [3], which establishes a compliant robot behavior with respect to external forces acting on it, and has the additional benefit in human–robot collaborative applications of allowing physical human guidance of the robot. Even though robot compliance effectively reduces the transferred energy from the robot to the operator during an accidental collision, additional safety features can be included to further protect the operators and to avoid contacts with their most sensitive surfaces. In the context of robot obstacle avoidance, Safety Control Barrier Functions (SCBFs) [4] have been gaining popularity in recent years [5]–[10], since they emphasize optimality and are minimally-invasive [11]. Recently, SCBFs have been used to adjust the Cartesian compliant behavior of a robot for obstacle avoidance with respect to its end-effector [5].

The authors are members of the ELLIIT Strategic Research Area at Lund University. This work was partially supported by the Wallenberg AI, Autonomous Systems and Software Program (WASP) and the Knut and Alice Wallenberg Foundation (KAW).

J. M. Salt Ducaju, julian.salt_ducaju@control.lth.se, B. Olofsson, A. Robertsson, and R. Johansson are with the Department of Automatic Control, LTH, Lund University, Lund, Sweden.

Moreover, when obstacle avoidance does not involve the Cartesian motion of the robot end-effector, but rather its link configuration, the main robot task needs not be modified. In this context, kinematic redundancy allows robotic manipulators to perform additional subtasks, such as obstacle avoidance, without modifying the robot behavior with respect to its main task by projecting the additional tasks in the null-space of the robot main task [12]. For this, a dynamic formulation that augments the Cartesian coordinates of the main robotic task by null-space velocities [13] is often used, since it allows decoupling of kinetic energies for each task. A compliant controller in the null-space of the robot main task based on the dynamic formulation in [13] was proposed in [14]. By avoiding inertia shaping, the controller in [14] avoided using feedback from the external forces and provided robustness with respect to model inaccuracies in the controller, while achieving a decoupling of the Cartesian and the null-space motion. Semi-definite Lyapunov functions were used in [14] to provide asymptotic stability guarantees for the null-space compliant motion. Nevertheless, stability guarantees for the variation of the stiffness and damping parameters for null-space compliant behavior have not been provided in this context so far.

Furthermore, obstacle avoidance is not the only beneficial subtask for HRC, and optimizing the robot joint configuration is also desirable, since it can maximize the robot manipulability, *e.g.*, by controlling that the angular positions of the robot joints are far from their limits [15]. An extension of [14] was presented in [16] for a hierarchical control structure with an arbitrary number of subtasks, where each additional subtask is projected on the null-space of the higher-priority tasks. However, the robots designed to perform collaborative tasks with humans (cobots) are usually built with 7 rotational joints, *e.g.*, the KUKA LBR iiwa robot or the Franka Emika Panda robot, and therefore, in robotic applications where the main task involves controlling the position and orientation of its end-effector, only one degree of freedom (DOF) would be available for additional subtasks. Then, it is not guaranteed that more than one subtask can be performed using the additional DOF with a hierarchical structure as in [16].

In this paper, we address the problem of improving safety in HRC for redundant robots by extending our previous work in [5] to contact-risk situations that do not involve the robot end-effector, but rather its link configuration. A joint impedance controller is projected in the null-space of the Cartesian robot motion to achieve a compliant motion toward a desired joint configuration, while keeping the main robotic

task unperturbed. The novelty of our proposal consists in using SCBFs to adjust the null-space compliant behavior of the robot for obstacle avoidance with respect to the body of the robot. In addition to improved safety, our proposed method should not affect the Cartesian robot end-effector motion nor require additional DOFs to be performed, since the SCBF-based obstacle avoidance shares the null-space DOF with the joint optimization subtask. A Lyapunov function is proposed to provide global asymptotic stability guarantees for varying the null-space compliant motion. Laboratory experiments have been performed for a collaborative assembly application to validate our method on a 7-DOFs manipulator.

The paper is organized as follows: Sec. II presents the kinematic and dynamic models used for redundant robotic manipulators. Then, Sec. III presents the nominal state-feedback controller, which is modified by a Quadratic Optimization (QP) problem presented in Sec. IV, where SCBFs are used as inequality constraints for obstacle avoidance. Section V explains the experiments performed for a collaborative assembly application and presents the results obtained. Finally, a discussion is included in Sec. VI and conclusions are drawn in Sec. VII.

II. Modeling for Redundant Robots

First, we review relevant kinematics and dynamics for redundant manipulators that show that the dynamics for the robot main task and for its null-space can be decoupled.

A. Kinematics for Redundant Robots

The kinematic relation between a robotic manipulator with n degrees of freedom (DOFs) and its main task in the m-dimensional task space is:

$$\xi = \mathcal{K}(q) \tag{1}$$

where $\xi \in \mathbb{R}^m$ represents the coordinates of the main robotic task and $q \in \mathbb{R}^n$ represents the coordinates of the joint space of the robot. Then, the manipulator Jacobian, $J(q) \in \mathbb{R}^{m\times n}$ is used to relate the main task velocity, $\dot{\xi}$, with respect to the joint velocity, $\dot{q}$:

$$\dot{\xi} = J(q)\dot{q} \tag{2}$$

where $J(q)$ is assumed to be of full rank throughout the presented work as in [17]. A robotic manipulator is considered to be kinematically redundant when $n > m$, and $r = n - m$ is called the degrees of redundancy.

A possible solution to the inverse kinematics for (2) is

$$\dot{q} = J_W^{\dagger}(q)\dot{\xi} + (I_n - J^{\mathrm{T}}(q)J_W^{\dagger\mathrm{T}}(q))\dot{q}_0 \tag{3}$$

where $\dot{q}_0 \in \mathbb{R}^n$ is an arbitrary vector in the robot joint space, $I_n \in \mathbb{R}^{n\times n}$ represents an identity matrix, and $J_W^{\dagger}(q)$ is the weighted generalized inverse

$$J_W^{\dagger}(q) = W^{-1}(q)J^{\mathrm{T}}(q)(J(q)W^{-1}(q)J^{\mathrm{T}}(q))^{-1} \tag{4}$$

with $W \in \mathbb{R}^{n\times n}$ being a symmetric positive definite matrix, $W \in S_{++}^n$. The second term of the right-hand side of (3) projects the arbitrary joint space vector $\dot{q}_0$ into the null-space of the main task, $\mathcal{N}(J)$, and it is necessary for a full decomposition of the joint motion in redundant manipulators.

Moreover, the velocity in the null-space of the main task can be rewritten by defining velocities $v_N \in \mathbb{R}^r$ [13], so

$$\dot{q}_{\mathrm{NS}} = (I_n - J^{\mathrm{T}}(q)J_W^{\dagger\mathrm{T}}(q))\dot{q}_0 = Z^{\mathrm{T}}(q)v_N \tag{5}$$

where $Z(q) \in \mathbb{R}^{r\times n}$ is composed by linearly independent vectors in $\mathcal{N}(J)$, $J(q)Z^{\mathrm{T}}(q) = 0$. Analogous to (2), the null-space velocities, v_N, can be related to the robot joint velocity by a Jacobian, $N(q) = (ZWZ^{\mathrm{T}})^{-1}ZW \in \mathbb{R}^{r\times n}$:

$$v_N = N(q)\dot{q} \tag{6}$$

Remark. *There might not exist compatible null-space coordinates, $s(q)$, such that $N(q) = \partial s(q)/\partial q$, so the null-space velocities, v_N, are, in general, not integrable [14].*

B. Dynamics for Redundant Robots

The rigid-body dynamics of the robot can be written in the joint space of the robot as [18]:

$$M(q)\ddot{q} + C(q,\dot{q})\dot{q} + G(q) = \tau + \tau^{\mathrm{ext}} \tag{7}$$

where $M(q) \in \mathbb{R}^{n\times n}$ is the generalized inertia matrix, $C(q,\dot{q}) \in \mathbb{R}^{n\times n}$ is the Coriolis matrix, $G(q) \in \mathbb{R}^n$ captures the gravity-induced torques, and $\tau \in \mathbb{R}^n$ represents the input torques. Finally, $\tau^{\mathrm{ext}} \in \mathbb{R}^n$ represents the external torques. For a kinematically redundant robot, the input torques can be decoupled as

$$\tau = \tau_\xi + \tau_{\mathrm{ns}} = J^{\mathrm{T}}(q)F_\xi + N^{\mathrm{T}}(q)F_N \tag{8}$$

where τ_ξ corresponds to the torques that are involved in the robot's main task, and τ_{ns} are torques acting in the null-space of the main task.

Moreover, if the weighting matrix W of the generalized inverse is chosen to be the generalized inertia matrix, M, $W = M$ in (4), the null-space torque, τ_{ns} in (8), does not cause an acceleration in the main task coordinates ξ [19]. Then, the task space is inertially decoupled from the minimal null-space motions, and the dynamics of each space can be considered separately:

$$M_\xi(q)\ddot{\xi} + C_\xi(q,\dot{q})\dot{\xi} + G_\xi(q) = F_\xi + F_\xi^{\mathrm{ext}} \tag{9}$$

$$M_N(q)\dot{v}_N + C_N(q,\dot{q})v_N + G_N(q) = F_N + F_N^{\mathrm{ext}} \tag{10}$$

However, to obtain fully-decoupled dynamics as in (9) and (10), a power-conserving feedback compensation on the centrifugal and Coriolis cross-terms should be included [14].

III. Nominal State-Feedback Controller

Consider a control-affine system:

$$\dot{x} = f(x) + g(x)u \tag{11}$$

that has closed-loop system dynamics with a state-feedback controller k according to:

$$\dot{x} = f_{cl}(x,t) = f(x) + g(x)k(x,t) \tag{12}$$

Then, the nominal state-feedback controller, $k = k^d$ in (12), should achieve the robot's desired behavior for human–robot collaboration: a Cartesian compliant behavior of the robot end-effector for safety, and possibly, human guidance, and a joint compliance behavior in the null-space of the main Cartesian task that increases the robot manipulability.

A. Main Task: Cartesian Impedance Control

A Cartesian impedance controller [3] is used to establish a mass-spring-damper relationship between the Cartesian pose variation of the robot end-effector from its reference, $\Delta\xi = \xi_D - \xi$ (ξ_D being the Cartesian reference), and the external Cartesian force, F_ξ^{ext}:

$$F_\xi^{\text{ext}} = M_\xi(q)\ddot{\xi} + (D + C_\xi(q,\dot{q}))\dot{\xi} - K\Delta\xi \tag{13}$$

where D and K are the virtual damping and stiffness matrices, respectively. The virtual inertia is chosen equal to the robot inertia, $M_\xi(q)$, to avoid inertia shaping [14]. The input force F_ξ, when the Cartesian external force is defined as in (13), should be equal to

$$F_\xi = K\Delta\xi - D\dot{\xi} + G_\xi(q) \tag{14}$$

B. Redundancy and Null-Space Motion

To obtain a compliant behavior in the null-space of the main task, the null-space component of the input torque, τ_{ns} in (8), can be chosen as a projection of a torque that contains a spring stiffness term, k_n, with respect to the joint position variation from its reference, $\Delta q = q_D - q$, and a damping term, d_n, for the null-space velocities, v_N [14]:

$$\tau_{\text{ns}} = N^{\text{T}}(q)k_n Z(q)\Delta q - N^{\text{T}}(q)d_n v_N \tag{15}$$

The desired joint configuration, q_D, is chosen as the closest configuration to the mid of the range of the joints, q_{mid}, where $\xi_D = p(q_D)$ to increase the robot manipulability. An optimization problem can be formulated to obtain q_D:

$$\begin{aligned} q_D = &\arg\ \min_{q_D\in\mathbb{R}^n} \frac{1}{2}\left|\left|q_D - q_{\text{mid}}\right|\right|_2^2 \\ &\text{s.t.}\ \ \xi_D = p(q_D) \end{aligned} \tag{16}$$

Then, the gravity-compensated closed-loop dynamics of the system obtained from (10) and using the decoupled torque input defined in (8) with (15) is

$$F_N^{\text{ext}} = M_N(q)\dot{v}_N + (d_n + C_N(q,\dot{q}))v_N - k_n Z(q)\Delta q \tag{17}$$

C. Controller Stability

The stability properties of the closed-loop system (13) and (17) have been studied in [14] using conditional stability and proposing a semi-definite Lyapunov function to show the asymptotic stability of the equilibrium point ($q = q_D$, $\dot{q} = 0$) for free-space motion. However, based on recent research that proved the global asymptotic stability for the main task (13) in a non-redundant robotic manipulator [5], we consider a strictly definite Lyapunov candidate function to provide a stronger proof of stability for the null-space motion:

Lemma III.1. *The Lyapunov function candidate*

$$V_{\text{ns}}(\Delta q, v_N) = \frac{1}{2}v_N^{\text{T}}M_N v_N + \frac{k_n}{2}\Delta q^{\text{T}}\Delta q - \alpha\Delta q^{\text{T}}Z^{\text{T}}M_N v_N \tag{18}$$

shows the global asymptotic stability of the null-space motion with input torque τ_{ns} in (15) for $\alpha > 0$ satisfying:

$$\min\left(\sqrt{\frac{k_n}{\lambda_{M,M_Z}}},\ \frac{2k_n}{d_n},\ \frac{d_n}{2(\lambda_{M,M_Z} + k_C||Z\Delta q||)}\right) > \alpha \tag{19}$$

where λ_{M,M_Z} is the largest eigenvalue of the matrix $Z^{\text{T}}M_N Z$, and k_C is a positive constant such that for all $w_1, w_2, w_3 \in \mathbb{R}^r$ [20]

$$||C_N(w_1, w_2)w_3|| \le k_C||w_2||||w_3|| \tag{20}$$

Proof: The detailed proof for the global asymptotic stability of the null-space motion has been omitted for conciseness since it is analogous to the proof of the stability of the Cartesian impedance controller in [5] but replacing $\Delta\xi$, $\dot{\xi}$, M_ξ, C_ξ, K, and D for Δq, v_N, M_N, C_N, k_n, and d_n, respectively. ■

IV. Quadratic Optimization

In this section, we modify the robot's null-space compliant behavior (17) of the nominal state-feedback controller k^d using a quadratic optimization problem that ensures that the robot states stay in a safe set to improve safety in HRC.

A. System Linearization

By applying partial feedback linearization [21, Ch. 9], the input, $u \in \mathbb{R}^n$, to the system in joint-space coordinates (7) can be written as the gravity-compensated joint torque:

$$u = \tau + \tau^{\text{ext}} - G(q) \tag{21}$$

Then, by choosing the state vector as $x = [q^{\text{T}}, \dot{q}^{\text{T}}]^{\text{T}} \in \mathbb{R}^{2n}$, the linearized system is

$$\dot{x} = A(q,\dot{q})x + B(q)u \tag{22}$$

where

$$A = \begin{bmatrix} 0_n & I_n \\ 0_n & -M^{-1}(q)C(q,\dot{q}) \end{bmatrix},\ B = \begin{bmatrix} 0_n \\ M^{-1}(q) \end{bmatrix} \tag{23}$$

B. Cost Function

Obstacle avoidance with respect to the body of the robot can be achieved without perturbing the robot main task if the additional torque required to avoid obstacles is applied in the null-space of the main task:

$$\Delta u = \Delta\tau_{\text{ns}} \tag{24}$$

Then, the compliance parameters of the joint torque (15) in the null-space projection of the main task can be varied to fulfill (24) so that the desired joint configuration q_D is not modified, thus achieving obstacle avoidance while allowing the optimization of the robot joint configuration:

$$\Delta\tau_{\text{ns}} = N^{\text{T}}(q)(-\Delta d_n v_N + \Delta k_n Z(q)\Delta q) \tag{25}$$

Therefore, a cost function that minimizes the value of the null-space stiffness and damping variation,

$$z = \begin{bmatrix}\Delta k_n & \Delta d_n\end{bmatrix}^{\text{T}} \tag{26}$$

can be formulated:

$$L(z) = \frac{1}{2}\left|\left|W_z z\right|\right|_2^2 \tag{27}$$

where a weighting matrix, $W_z \in \mathbb{R}^{2\times2}$, is used to select the desired ratio between the null-space stiffness and damping variations. Since $W_z \in S^2_{++}$ yields $Q \in S^2_{++}$, Q being the quadratic term of the cost function (27), W_z may be chosen as:

$$W_z = \begin{bmatrix} 1 & 0 \\ 0 & \beta \end{bmatrix} \tag{28}$$

for $\beta \in \mathbb{R}_{>0}$. Then, if $\beta > 1$ the variation of the stiffness is prioritized and if $\beta < 1$ the damping variation is prioritized. In addition, selecting (27) as the cost function to be solved in the QP problem yields a minimal variation of the input torque to the robot, $\Delta\tau_{\text{ns}}$ of Eq. (25), thus minimizing the difference between the system input u and the nominal state-feedback k^d.

C. Inequality Constraint for Obstacle Avoidance

An inequality constraint for the input of the linearized system (22)

$$A_{\text{BF}} u \leq b_{\text{BF}} \tag{29}$$

can be used to ensure that the body of the robot stays within a safety distance of an obstacle by guaranteeing the forward invariance of a safe (*i.e.*, uncollided) set of robot states [11]:

Theorem IV.1. *A safe set $\mathcal{C} = \{x \in \mathbb{R}^{2n} \mid h(x) \geq 0\}$ is forward invariant if*

$$\sup_{u\in\mathcal{U}} [L_f h(x) + L_g h(x) u] \geq -\kappa(h(x)) \tag{30}$$

for all $x \in \mathcal{D}$, h being the Safety Control Barrier Function (SCBF), $h : \mathcal{D} \to \mathbb{R}$ with $\mathcal{C} \subseteq \mathcal{D} \subset \mathbb{R}^{2n}$, κ an extended class-$\mathcal{K}_\infty$ function (strictly monotonically increasing), $L_f h(x) = {}^{\partial h}/_{\partial x} f(x)$, and $L_g h(x) = {}^{\partial h}/_{\partial x} g(x)$ [11].

Therefore, a safety function has been formulated so that the safety distance is always greater than or equal to the current distance from the robot to the obstacle subtracted by the distance needed to brake the system into a full stop with constant and instantaneous acceleration [5], [6], [22]. Moreover, to avoid having a computationally-expensive calculation of the distance between the robot and the obstacle, each link of the robot geometry is simplified using basic geometric models, such as capsules, which have recently gained popularity [7], [23] for fitting well to the shape of a robotic manipulator (see Fig. 1).

Then, for each link $i \in \{1, \ldots, n\}$, the SCBF, $h_i : \mathcal{D} \to \mathbb{R}$, that enforces obstacle avoidance is, as in [5], [6], [22]:

$$h_i(x) = \sqrt{2a_{\text{br}}(||\Delta\rho_i|| - D_{s,i})} + \frac{\Delta\rho_i^{\text{T}}}{||\Delta\rho_i||} J_i \dot{q} \tag{31}$$

with $\Delta\rho_i = \rho_i - \rho_o$ being the distance between the closest point to the obstacle in the i-th link, ρ_i, and the obstacle's position ρ_o, and $J_i \in \mathbb{R}^{3\times n}$ being a Jacobian that relates the linear velocity of the selected point in the i-th link, ρ_i, with the angular velocity of the joints $\dot{q}$. Also, the safety distance, $D_{s,i} = r_{r,i} + r_o$, uses $r_{r,i}$ and r_o as protective distances around the link i and the obstacle, respectively, and $a_{\text{br}} > 0$ denotes the robot braking acceleration. Moreover, the second term of the right-hand side of (31) is equivalent to the relative velocity, $v_{\text{re},i}$ of ρ_i with respect to ρ_o, as shown in Fig. 1.

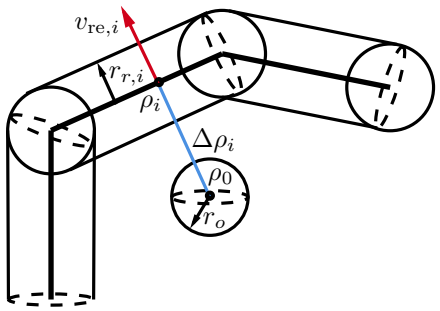

Fig. 1. Illustration of the capsules model [7], [23] (for a 3-link robot) used to determine the safety distance. The blue line represents the distance, $\Delta\rho_i$, between the obstacle's position, ρ_0, and its closest point within the i-th link of the robot, ρ_i. The red arrow represents the relative velocity, $v_{\text{re},i}$, of ρ_i with respect to the obstacle ρ_0 and $r_{r,i}$, r_o are the safety distances around the robot's i-th link and the obstacle, respectively.

Considering the system model (22), (23) and choosing the inequality constraint that must be satisfied to ensure that the safe set is forward invariant (30) as $\dot{h}(x) + \gamma h^\omega \geq 0$ [22], the elements in (29) are for each link i equal to

$$A_{\text{BF,i}} = -\Delta\rho_i^{\text{T}} J_i M^{-1} \tag{32}$$

$$\begin{aligned} b_{\text{BF,i}} = {} & \frac{a_{\text{br}} \Delta\rho_i^{\text{T}} \left[0_{3\times n},\, J_i\right] x}{\sqrt{2a_{\text{br}}(||\Delta\rho_i|| - D_{s,i})}} + \left|\left| \left[0_{3\times n},\, J_i\right] x \right|\right|^2 \\ & - \frac{\left(\Delta\rho_i^{\text{T}} \left[0_{3\times n},\, J_i\right] x\right)^2}{||\Delta\rho_i||^2} + ||\Delta\rho_i|| \gamma h_i^\omega \\ & + \Delta\rho_i^{\text{T}} \left[0_{3\times n},\, \dot{J}_i - J_i M^{-1} C\right] x \end{aligned} \tag{33}$$

Therefore, the inequality constraint (29) in z (26) is equivalent to

$$A'_{\text{BF}} z \leq b'_{\text{BF}} \tag{34}$$

for $A'_{\text{BF}} = A_{\text{BF}} N^{\text{T}} \left[Z\Delta q,\, -v_N\right]$ and $b'_{\text{BF}} = b_{\text{BF}} - A_{\text{BF}} k^d$.

D. Stable Variation of the Null-Space Compliant Behavior

The strict stability of the null-space motion has previously been shown in Lemma III.1 for constant null-space stiffness and damping parameters. Also, analogous to the passivity condition shown for a Cartesian impedance controller in [5], since $M_N, k_n, d_n \in S_{++}$, a passive map from the null-space external force, F_N^{ext}, to the null-space velocity, v_N, was guaranteed:

$$\dot{V}_{\text{ns}} < v_N^{\text{T}} F_N^{\text{ext}} \tag{35}$$

with $\dot{V}_{\text{ns}}$ being the time-derivative of the Lyapunov function (18) with constant null-space stiffness and damping terms.

However, if these compliance parameters vary with time, additional terms $\Delta\dot{V}_{\text{ns}}(t)$, which may break the passivity of the system, appear in the time-derivative of the Lyapunov function used for the stability proof of the null-space motion:

$$\dot{V}'_{\text{ns}}(t) = \dot{V}_{\text{ns}} + \Delta\dot{V}_{\text{ns}}(t) \tag{36}$$

with $\dot{V}'_{\text{ns}}(t)$ being the time-derivative of the Lyapunov function with time-varying terms. The additional terms are equal

to

$$\Delta\dot{V}_{\rm ns}(t) = -\frac{\Delta d_n}{2}\left[v_N - \alpha Z\Delta q\right]^{\rm T}\left[v_N - \alpha Z\Delta q\right] + \frac{\dot{k}_n}{2}\Delta q^{\rm T}\Delta q \tag{37}$$

Moreover, energy-based virtual storage methods can be used to guarantee the passivity of the system by controlling that the amount of energy introduced to the robotic manipulator for varying the stiffness of the robot is lower than the energy dissipated by itself [24], [25]. Being T the energy stored in a virtual reservoir, the total energy of the system composed by the robot and the virtual storage is equal to $W_{\rm ns} = T + V'_{\rm ns} > 0$, with $\dot{W}_{\rm ns} < 0$. Then, the only additional condition needed to ensure the passivity of the system is that there is enough energy in the storage. For a time interval $\left[t_s, t_f\right]$, this condition is [25]:

$$T(t_f) = T(t_s) + \int_{t_s}^{t_f} P_D d\tau - \int_{t_s}^{t_f} P_K d\tau \geq \delta \tag{38}$$

with δ being the minimum amount of energy allowed in the storage. Also, P_D and P_K represent the dissipated power due to damping and the power caused by stiffness variation, respectively,

$$P_D = \frac{d_n + \Delta d_n}{2}\left[v_N - \alpha Z\Delta q\right]^{\rm T}\left[v_N - \alpha Z\Delta q\right] \tag{39}$$

$$P_K = \frac{\dot{k}_n}{2}\Delta q^{\rm T}\Delta q \tag{40}$$

Then, the condition to ensure that the energy storage used to guarantee the passivity of the system does not get empty (38) can be rewritten as an inequality constraint:

$$A_{\rm T} z \leq b_{\rm T} \tag{41}$$

with

$$A_{\rm T} = \begin{bmatrix} \frac{1}{2}\Delta q^{\rm T}\Delta q \\ -\frac{t_f - t_s}{2}\left[v_N - \alpha Z\Delta q\right]^{\rm T}\left[v_N - \alpha Z\Delta q\right] \end{bmatrix}^{\rm T} \tag{42}$$

$$b_{\rm T} = d_n\frac{t_f - t_s}{2}\left[v_N - \alpha Z\Delta q\right]^{\rm T}\left[v_N - \alpha Z\Delta q\right] + \frac{\Delta k_n(t_s)}{2}\Delta q^{\rm T}\Delta q + T(t_s) - \delta \tag{43}$$

Additionally, the positive-definiteness of the null-space stiffness and damping, *i.e.*, $k_n + \Delta k_n(t) \in S_{++}$ and $d_n + \Delta d_n(t) \in S_{++}$, are necessary conditions to show the stability of the null-space motion using Lemma III.1. These conditions can be enforced by rewriting them as:

$$A_{\rm kd} z < b_{\rm kd} \tag{44}$$

with $A_{\rm kd} = -I_2$ and $b_{\rm kd} = \begin{bmatrix} k_n & d_n \end{bmatrix}^{\rm T}$.

E. Quadratic Optimization Problem Summary

Finally, the resulting optimization problem to modify the nominal state-feedback controller for obstacle avoidance is:

$$\begin{aligned} z = \arg\ &\min\nolimits_{z\in\mathbb{R}^2} L(z) \\ \text{s.t.}\ \ & A'_{\rm BF} z \leq b'_{\rm BF} \\ & A_{\rm kd} z < b_{\rm kd} \\ & A_{\rm T} z \leq b_{\rm T} \end{aligned} \tag{45}$$

V. Experiments

In this section, we provide an experimental evaluation of the proposed method for an assembly application.

A. Experimental Setup

The experimental validation consisted in a collaborative assembly of an emergency button using a redundant robotic manipulator, Franka Emika Panda [26], as seen in Fig. 2. This assembly process consisted of three events. First, while the robot snapped the switch into the bottom box [27], the human operator secured the pusher to the top box with a small plastic nut. Finally, the robot joined the top and bottom boxes.

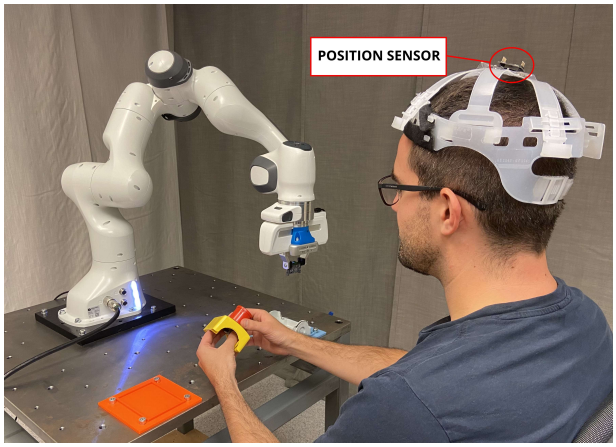

Fig. 2. Experimental setup for the collaborative assembly of an emergency button.

A Cartesian compliance controller was implemented to allow the operators to interact with the position and orientation of the robot arm to correct any robot malfunction, and also to allow a careful handling of the assembly pieces, while a null-space compliance controller optimized the robot joint configuration. However, to increase safety in the most sensitive parts of the operator's body, *i.e.*, its head, the operator wore a helmet, which was equipped with a position sensor (see Fig. 2). Then, the null-space compliance parameters were varied based on the optimization problem in (45) to avoid any collision between the body of the robot and the operator's head.

B. Results

The results for a situation where a potential collision was avoided during the assembly event in which the robot joined the top and the bottom of the box are shown in Figs. 3 and 4 and in Table I. First, it is seen in Fig. 3 how the safety control barrier function $h_{\rm min} = \min(h_i)\ \forall\ i \in \{1, \ldots, n\}$ had a positive value throughout this motion, thus the states of the robot stayed inside the safe set $\mathcal{C}$. Also, the inequality constraint (34) of the QP problem (45) was active between $t = 1.18$ s and $t = 3.91$ s, which caused the variation of the null-space stiffness $k_n + \Delta k_n$ and damping $d_n + \Delta d_n$, so that the forward invariance condition of the safe set $\mathcal{C}$ (30) was fulfilled.

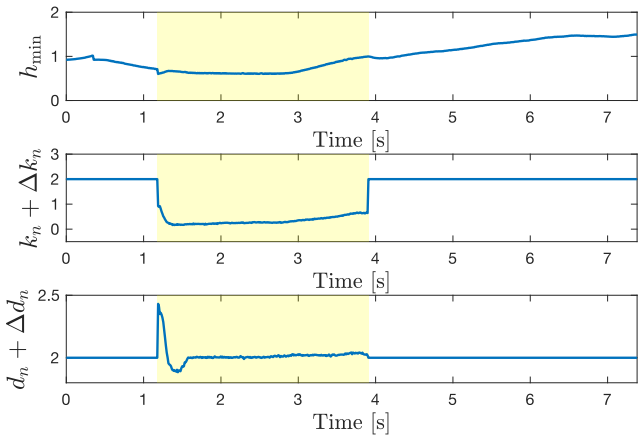

Fig. 3. Temporal evolution of the barrier function $h_{\min}$, the null-space stiffness $k_n + \Delta k_n$, and the null-space damping $d_n + \Delta d_n$. The yellow background indicated the time interval when the inequality constraint (34) of the QP problem (45) was active.

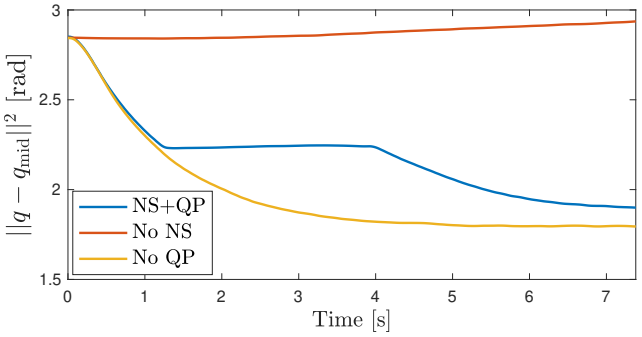

Fig. 4. Temporal evolution of the L_2-norm of the difference between the joint configuration q and the midpoint configuration q_{mid}.

Moreover, Table I shows relevant performance metrics for the highest-risk situation, defined as the time instant where the safety control barrier function $h_{\min}$ was the closest to zero. As seen in Table I, the highest-risk situation occurred at $t = 1.19$ s, where the minimum distance between the operator's head and the body of the robot, $D_{\min}$, was equal to 0.25 m. It is also shown in Table I that the time-to-collision, TTC, defined as the time that would elapse until a collision occurred for a constant relative velocity between the operator's head and the robot's body, was equal to 0.37 s, which highlights the minimally-invasive features of the proposed method.

TABLE I

PERFORMANCE METRICS FOR THE HIGHEST-RISK SITUATION

Time (t)	Minimum Distance ($D_{\min}$)	Time-to-Collision (TTC)
1.19 s	0.25 m	0.37 s

Furthermore, Fig. 4 shows the temporal evolution of the L_2-norm of the difference between the joint configuration q and the midpoint configuration q_{mid} for the developed controller (*NS+QP*) compared to the cases where no null-space motion was implemented (*No NS*) and where no null-space compliance variation was used (*No QP*). The implementation of null-space motion could effectively be used to decrease the difference between the robot configuration and the midpoints of the robot joints' ranges to increase the robot manipulability. Also, since there was only one DOF available in the null-space of the main (Cartesian) task, the controller was able to increase the robot manipulability as long as it did not conflict with the safety condition in (34).

VI. DISCUSSION

Several authors have used SCBFs for obstacle avoidance in robotic manipulators [5]–[10]. However, these previous works focused on non-redundant robots, and therefore, obstacle avoidance would modify the main robotic task. The novelty of the method presented here is that we consider redundant robots and use their additional DOFs to apply the necessary joint torque variation in the null-space of the robot's main task in a dynamically consistent way such that this main robotic task is not altered unnecessarily. Further, it is straightforward to combine the proposed method with previous proposals that achieved obstacle avoidance with respect to the robot end-effector, such as [5], thus achieving a safe robot behavior in any contact-risk situation.

Moreover, the use of the null-space projection of the main robotic task for obstacle avoidance has been studied in the past [28]. However, artificial potential field methods [29] were used in these works. The main benefits of using SCBFs instead of artificial potential fields were discussed in [5], *i.e.*, SCBFs only modify the nominal behavior of the system when necessary. Additionally, the use of SCBFs in our formulation allows to explicitly take the dynamics of the robot into consideration when formulating the SCBF to guarantee adherence to the constraints [5], [8], thus avoiding potential constraint violations that may occur when only considering the robot kinematics in the formulation of SCBFs [6], [7], [10], as illustrated by [9].

Furthermore, the proposed null-space compliance-varying controller achieved shared use of the only DOF available in the null-space of the main robot task, simultaneously, for obstacle avoidance and for the increase of the robot manipulability, thus benefiting human–robot collaborative applications. Also, the desired joint configuration in the proposed null-space controller was chosen as the closest configuration to the midpoints of the joints being $\xi_D = p(q_D)$. An alternative choice of desired joint configuration could be one where a performance index, such as the manipulability index [17], [30], is maximized. However, depending on the task being executed, the manipulability index in [17], [30] could be locally maximized close to a joint limit, leaving little or no margin for human guidance. In addition, the condition $\xi_D = p(q_D)$ used to set the null-space compliant behavior of the robot ensures the global asymptotic stability of the null-space motion based on Lemma III.1 [14].

Additionally, showing stability proofs for the null-space compliant motion of a robotic manipulator is challenging. In [14], the authors used the concept of conditional stability

to propose a semi-definite Lyapunov function to prove the asymptotic stability of null-space motion. Our contribution consisted in adding a cross-term to the Lyapunov function candidate, in the same fashion as it was done in [5], [20] for non-redundant manipulators, to provide a stronger stability proof, *i.e.*, global asymptotic stability of the null-space motion. In addition, the stability of the variation of the null-space stiffness and damping coefficients has been shown by using a passive-energy storage method [24], as was done in [5] for Cartesian impedance control.

Finally, an interesting novelty of the here presented work with respect to [5] is that the optimization problem is formulated with the variation of the compliance parameters as the optimization variables, which allowed us to express the necessary conditions for stability as inequality constraints (41), (44) of the QP problem, as well as ensured that the quadratic term of the QP problem is positive definite. Also, even though it has not been observed for the experiments described in Sec. V, a hypothetical infeasibility of the QP problem would indicate the conditions for which a safety shutdown of the null-space motion was required, *e.g.*, if stability could not be ensured.

VII. Conclusion

Safety in human–robot collaborative applications can be improved in a stable manner while keeping the main robotic Cartesian task unperturbed. For this, we proposed to modify the joint compliant behavior of a redundant robot projected in the null-space of the Cartesian task using SCBFs. In experiments with a 7-DOFs robot for a collaborative assembly application, we demonstrated that safety can be improved simultaneously to the optimization of the robot joint configuration in a single DOF.

References

[1] C. Schou, J. Damgaard, S. Bøgh, and O. Madsen, "Human-robot interface for instructing industrial tasks using kinesthetic teaching," in *IEEE International Symposium on Robotics (ISR)*, Seoul, Korea, Oct. 19–27, 2013, pp. 1–6.

[2] N. Kousi, G. Michalos, S. Aivaliotis, and S. Makris, "An outlook on future assembly systems introducing robotic mobile dual arm workers," *Procedia CIRP*, vol. 72, pp. 33–38, 2018.

[3] N. Hogan, "Impedance control: An approach to manipulation: Parts I–III," *Journal of Dynamic Systems, Measurement, and Control*, vol. 107, no. 1, pp. 1–24, 1985.

[4] A. Forsgren, P. E. Gill, and M. H. Wright, "Interior methods for nonlinear optimization," *SIAM Review*, vol. 44, no. 4, pp. 525–597, 2002.

[5] J. M. Salt-Ducaju, B. Olofsson, A. Robertsson, and R. Johansson, "Robot Cartesian compliance variation for safe kinesthetic teaching using safety control barrier functions," in *IEEE International Conference on Automation Science and Engineering (CASE)*, Mexico City, Mexico, Aug. 20–24, 2022.

[6] F. Ferraguti, M. Bertuletti, C. T. Landi, M. Bonfè, C. Fantuzzi, and C. Secchi, "A control barrier function approach for maximizing performance while fulfilling to ISO/TS 15066 regulations," *IEEE Robotics and Automation Letters*, vol. 5, no. 4, pp. 5921–5928, 2020.

[7] C. T. Landi, F. Ferraguti, S. Costi, M. Bonfè, and C. Secchi, "Safety barrier functions for human-robot interaction with industrial manipulators," in *European Control Conference (ECC)*, Naples, Italy, Jun. 25–28, 2019, pp. 2565–2570.

[8] M. Rauscher, M. Kimmel, and S. Hirche, "Constrained robot control using control barrier functions," in *IEEE/RSJ International Conference on Intelligent Robots and Systems (IROS)*, Daejeon, Korea, Oct. 9–14, 2016, pp. 279–285.

[9] A. Singletary, S. Kolathaya, and A. D. Ames, "Safety-critical kinematic control of robotic systems," *IEEE Control Systems Letters*, vol. 6, pp. 139–144, 2021.

[10] F. Benzi and C. Secchi, "An optimization approach for a robust and flexible control in collaborative applications," in *IEEE International Conference on Robotics and Automation (ICRA)*, Xi'an, China, 31 May–4 Jun. 2021, pp. 3575–3581.

[11] A. D. Ames, S. Coogan, M. Egerstedt, G. Notomista, K. Sreenath, and P. Tabuada, "Control barrier functions: Theory and applications," in *European Control Conference (ECC)*, Naples, Italy, Jun. 25–28, 2019, pp. 3420–3431.

[12] J. M. Salt-Ducaju, B. Olofsson, A. Robertsson, and R. Johansson, "Joint stiction avoidance with null-space motion in real-time model predictive control for redundant collaborative robots," in *IEEE International Conference on Robot and Human Interactive Communication (RO-MAN)*, Aug. 8–12, 2021, pp. 307–314.

[13] J. Park, "Analysis and control of kinematically redundant manipulators: An approach based on kinematically decoupled joint space decomposition," Ph.D. dissertation, Dpt. Mech. Eng., Pohang University of Science and Technology, 2000, Doc. No. 991000372949703286.

[14] C. Ott, A. Kugi, and Y. Nakamura, "Resolving the problem of non-integrability of nullspace velocities for compliance control of redundant manipulators by using semi-definite Lyapunov functions," in *IEEE International Conference on Robotics and Automation (ICRA)*, Pasadena, CA, USA, May 19–23, 2008, pp. 1999–2004.

[15] Y. Nakamura, *Advanced robotics: Redundancy and optimization*. Addison-Wesley, Reading, MA, USA, 1990.

[16] A. Dietrich, C. Ott, and A. Albu-Schäffer, "Multi-objective compliance control of redundant manipulators: Hierarchy, control, and stability," in *IEEE/RSJ International Conference on Intelligent Robots and Systems (IROS)*, Tokyo, Japan, Nov. 3–7, 2013, pp. 3043–3050.

[17] O. Khatib, "A unified approach for motion and force control of robot manipulators: The operational space formulation," *IEEE Journal on Robotics and Automation*, vol. 3, no. 1, pp. 43–53, 1987.

[18] B. Siciliano and O. Khatib, *Springer Handbook of Robotics*. Springer, Berlin, Germany, 2016.

[19] O. Khatib, "Inertial properties in robotic manipulation: An object-level framework," *International Journal of Robotics Research*, vol. 14, no. 1, pp. 19–36, 1995.

[20] V. Santibáñez and R. Kelly, "Strict Lyapunov functions for control of robot manipulators," *Automatica*, vol. 33, no. 4, pp. 675–682, 1997.

[21] H. K. Khalil, *Nonlinear control*. Pearson Higher Ed., New York, USA, 2014.

[22] L. Wang, A. D. Ames, and M. Egerstedt, "Safety barrier certificates for collisions-free multirobot systems," *IEEE Transactions on Robotics*, vol. 33, no. 3, pp. 661–674, 2017.

[23] H.-C. Lin, C. Liu, Y. Fan, and M. Tomizuka, "Real-time collision avoidance algorithm on industrial manipulators," in *Conference on Control Technology and Applications (CCTA)*, Kohala Coast, HI, USA, Aug. 27–30, 2017, pp. 1294–1299.

[24] F. Ferraguti, C. Secchi, and C. Fantuzzi, "A tank-based approach to impedance control with variable stiffness," in *IEEE International Conference on Robotics and Automation (ICRA)*, Karlsruhe, Germany, May 6–10, 2013, pp. 4948–4953.

[25] C. T. Landi, F. Ferraguti, C. Fantuzzi, and C. Secchi, "A passivity-based strategy for coaching in human-robot interaction," in *IEEE International Conference on Robotics and Automation (ICRA)*, Brisbane, Australia, May 21–25, 2018, pp. 3279–3284.

[26] Franka Emika, "Franka Emika Panda – Data Sheet," https://www.generationrobots.com/media/panda-franka-emika-datasheet.pdf, 2019, (Visited on 2022-09-13).

[27] A. Stolt, M. Linderoth, A. Robertsson, and R. Johansson, "Force controlled assembly of emergency stop button," in *IEEE International Conference on Robotics and Automation (ICRA)*, Shanghai, China, May 9–13, 2011, pp. 3751–3756.

[28] H.-C. Lin, Y. Fan, T. Tang, and M. Tomizuka, "Human guidance programming on a 6-DOF robot with collision avoidance," in *IEEE/RSJ International Conference on Intelligent Robots and Systems (IROS)*, Daejeon, Korea, Oct. 9–14, 2016, pp. 2676–2681.

[29] O. Khatib, "Real-time obstacle avoidance for manipulators and mobile robots," in *IEEE International Conference on Robotics and Automation (ICRA)*, vol. 2, St. Louis, USA, Mar. 25–28, 1985, pp. 500–505.

[30] Y. Oh, W. Chung, and Y. Youm, "Extended impedance control of redundant manipulators based on weighted decomposition of joint space," *Journal of Robotic Systems*, vol. 15, no. 5, pp. 231–258, 1998.